Delayed sudden death of entanglement at exceptional points

Subhadeep Chakraborty* and Amarendra K. Sarma†
Department of Physics, Indian Institute of Technology Guwahati, Guwahati 781039, Assam, India

(Received 2 June 2019; published 27 December 2019)

Almost a decade ago, physicists encountered a strange quantum phenomenon that predicts an unusual death of entanglement, under the influence of a local noisy environment, known as entanglement sudden death (ESD). This could be an immediate stumbling block in realizing all entanglement based quantum information and computation protocols. In this paper, we propose a scheme to tackle such shortcomings by exploiting the phenomenon of exceptional points. Starting with a binary mechanical $\mathcal{PT}$ symmetric system, realized over an optomechanical platform, we show that a substantial delay in ESD can be achieved via pushing the system towards an exceptional point. This finding has been further extended to a higher-order (third-order) exceptional point by taking a more complicated tripartite entanglement into account.

DOI: 10.1103/PhysRevA.100.063846

I. INTRODUCTION

$\mathcal{PT}$ symmetric quantum mechanics, as an extension of standard quantum theory into the complex domain, was introduced by Bender and Boettcher in 1998. Followed by their seminal papers [1,2], this whole new class of non-Hermitian Hamiltonians was established that could exhibit a spectrum of entirely real eigenvalues under the only restriction $[H, \mathcal{PT}] = 0$ [3]. Here, $\mathcal{P}$ refers to the parity operator that simply interchanges two of the constituent modes of the system, while $\mathcal{T}$ is the time-reversal operator that takes $i \to -i$. A more striking feature of such Hamiltonians is the breaking of $\mathcal{PT}$ symmetry, in which the eigenspectrum switches from being entirely real to being completely imaginary. Such an abrupt $\mathcal{PT}$ phase transition is marked by the presence of an exceptional point (EP) [4,8] where two (or more) eigenvalues and their corresponding eigenvectors coalesce and become degenerate.

While the search for $\mathcal{PT}$ symmetric devices is on, it occurs that one can easily implement such notions by judiciously providing gain and loss to an optical system. This leads to a remarkable exploration of $\mathcal{PT}$ phase transitions, in particular to photonic systems, such as optical waveguides [5–8], lattices, and resonators [9–12]. Moreover, based on these realizations, the existence of EPs has further triggered many exotic phenomena, including nonreciprocal light propagation [10], laser mode control [11–14], unidirectional invisibility [9,15–17], optical sensing [18–20], light stopping [21], and structuring [22].

At this point, one must note that most of these studies explored so far are confined in the so-called classical regime, as the involved components are essentially macroscopic in nature. Therefore, any $\mathcal{PT}$ symmetric device the dynamics of which is governed by an intrinsic quantum-mechanical equation of motion would provide a better insight into this theory. Along this direction, researchers have proposed a few architectures, including cold atoms [23,24], Bose-Einstein condensates [25], optomechanical devices [26–28], and recent circuit QED systems [29]. These quantum $\mathcal{PT}$ symmetric devices allow us to explore many intrinsic quantum properties, such as critical phenomena [30], entanglement [31], chiral population transfer [32,33], decoherence dynamics [34], and information retrieval and criticality [35]. However, the true quantumness of a $\mathcal{PT}$ symmetric device still remains questionable, as while dealing with such gain (amplifying) and cooling (dampening) mechanisms one often abandons the associated quantum noises which rather must exist to preserve the proper commutation relation. So far, $\mathcal{PT}$ symmetry including quantum noises has been attempted in a very few studies [36–39], which indicate a drastic difference from the usual (without considering quantum noises) predictions. Notably, in Ref. [40], it has been shown that the continuous variable (CV) entanglement generated in a system of two coupled waveguides is seriously affected owing to the presence of quantum noises. Recently, incorporating gain saturation, it is proposed to reduce the influence of quantum noise [41] on entanglement.

Entanglement [42], being a form of correlation that is inherent to quantum systems, has become an invaluable resource for futuristic quantum computation and communication protocols. However, for a real-world implementation of such schemes, the longevity of the available entanglement is what experimentalists are mostly concerned about, as it is now well understood that any unavoidable interaction with an external environment brings noise to the system which is substantially detrimental to the generated entanglement. One such destructive manifestation is entanglement sudden death (ESD) [43], where the system loses entanglement in finite time. This unfortunate fate of entanglement has been both theoretically predicted and experimentally verified in a wide variety of entangled pairs involving atoms [44], photons [45], spin chains [46], and continuous Gaussian states [47,48]. Therefore, any manipulation that either avoids or delays ESD will help in executing various quantum

*c.subhadeep@iitg.ac.in
†aksarma@iitg.ac.in

information processing (QIP) protocols, that would otherwise be spoiled by the short entanglement lifetime. To overcome such shortcomings, a number of distinctive proposals have been put forward, such as quantum error correction [49,50], local unitary operation [51,52] dynamical decoupling [53,54], decoherence free subspace [55,56], the quantum Zeno effect [57,58], delayed choice of decoherence suppression [59], and quantum measurement reversal [60–62].

In this paper, we investigate the phenomenon of death of entanglement under the $\mathcal{PT}$ symmetric scenario. To the best of our knowledge, entanglement in $\mathcal{PT}$ symmetric geometries has been mostly dealt with in optical binary systems, around the canonical $\mathcal{PT}$ phase transition point (EP). Therefore, it is intriguing to ask the following question: what happens to the entanglement evolution if one goes beyond the standard bipartite model to a more involved multipartite configuration, possessing a higher-order exceptional point? To answer this question, we consider binary and ternary mechanical $\mathcal{PT}$ symmetric systems, individually, within an optomechanical setup. In particular, to engineer the mechanical gain and loss into these systems, we exercise a similar approach of first tuning the cavity to the Stokes and anti-Stokes sidebands, followed by an adiabatic elimination of the cavity field. However, unlike the previous reports [27,63], here we take the full quantum noises into account. Interestingly, we find that in both the cases the entanglement death can be substantially slowed down in the close vicinity of the exceptional points. This conclusion is further supported by analyzing the time evolution of two-mode Wigner functions near the EP. Finally, we discuss the effect of thermal noise on the bipartite and the tripartite entanglement evolution.

The rest of this paper is organized as follows. In Sec. II, we start with a detailed derivation of the optomechanically induced gain and loss rate in a mechanical resonator. Then, in Sec. III, we construct the reduced binary $\mathcal{PT}$ symmetric model and investigate the entanglement behavior, while approaching to an exceptional point. This is followed in Sec. IV by an investigation of tripartite entanglement evolution in the ternary $\mathcal{PT}$ symmetric setup, possessing a third-order exceptional point. Finally, we conclude in Sec. V.

II. CAVITY OPTOMECHANICS BASED ARCHITECTURE TO REALIZE THE GAIN AND LOSS IN A MECHANICAL SYSTEM

In this section, we outline the derivation of the optomechanically induced gain and loss in an mechanical system. To begin with, we first consider a generic cavity optomechanical system [64], consisting of a single cavity mode of frequency ω_c and a mechanical mode of frequency ω_m. Following a rotating frame transformation at a (laser) frequency ω_l, the Hamiltonian of this system reads as ($\hbar = 1$)

$$H = \Delta_0 a^\dagger a + \omega_m b^\dagger b - g a^\dagger a(b^\dagger + b) + E_0(a^\dagger + a), \quad (1)$$

where a ($a^\dagger$) and b ($b^\dagger$) are, respectively, the annihilation (creation) operators of the cavity field and the mechanical resonator. g is the strength of the single-photon optomechanical coupling, and E_0 is the driving amplitude with $\Delta_0 = \omega_c - \omega_l$ being the cavity detuning. Taking the fluctuation and dissipation processes into account, the dynamics of the system is then fully described by the following set of nonlinear quantum Langevin equations (QLEs):

$$\dot{a} = -(i\Delta_0 + \kappa/2)a + iga(b^\dagger + b) - iE_0 + \sqrt{\kappa}a^{\rm in}, \quad (2a)$$

$$\dot{b} = -(i\omega_m + \gamma/2)b + iga^\dagger a + \sqrt{\gamma}b^{\rm in}, \quad (2b)$$

where κ (γ) is the cavity decay (mechanical damping) rate. $a^{\rm in}$ is the zero-mean vacuum input noise operator, satisfying the only nonzero correlation function $\langle a_{\rm in}(t)a_{\rm in}^\dagger(t')\rangle = \delta(t-t')$, and $b^{\rm in}$ refers to the random Brownian noise operator, with zero-mean value and Markovian correlation functions, given by $\langle b^{\rm in^\dagger}(t)b^{\rm in}(t')\rangle = n_{\rm th}\delta(t-t')$, $\langle b^{\rm in}(t)b^{\rm in^\dagger}(t')\rangle = (n_{\rm th}+1)\delta(t-t')$. Here, the parameter $n_{\rm th} = [\exp(\frac{\hbar\omega_m}{k_B T}) - 1]^{-1}$ denotes the mean thermal phonon number at temperature T (k_B being the Boltzmann constant).

For a strongly driven cavity, we now adopt the standard linearization technique and expand each of these operators as a sum of its c-number classical steady-state value plus a time-dependent zero-mean quantum fluctuation operator, i.e., $a(t) \to \alpha + a(t)$ and $b(t) \to \beta + b(t)$. These steady-state values can then be obtained by solving the following nonlinear algebraic equations:

$$(i\Delta + \kappa/2)\alpha + iE_0 = 0, \quad (3a)$$

$$(i\omega_m + \gamma_m/2)\beta - ig|\alpha|^2 = 0, \quad (3b)$$

where $\Delta = \Delta_0 - 2g{\rm Re}(\beta)$ is the effective cavity detuning. On the other hand, the dynamics of the quantum fluctuations are given by the linearized QLEs (valid in the limit of $|\alpha| \gg 1$), written as

$$\dot{a} = -(i\Delta + \kappa/2)a + iG(b^\dagger + b) + \sqrt{\kappa}a^{\rm in}, \quad (4a)$$

$$\dot{b} = -(i\omega_m + \gamma/2)b + iG(a^\dagger + a) + \sqrt{\gamma}b^{\rm in}, \quad (4b)$$

with $G = g|\alpha|$ being the effective many-photon optomechanical coupling strength.

Next, we introduce two slowly varying operators, $\tilde{a} = ae^{i\Delta t}$ and $\tilde{b} = be^{i\omega_m t}$, and rewrite Eq. (4) in the following manner:

$$\dot{\tilde{a}} = -\frac{\kappa}{2}\tilde{a} + iG(\tilde{b}^\dagger e^{i(\Delta+\omega_m)t} + \tilde{b}e^{i(\Delta-\omega_m)t}) + \sqrt{\kappa}\tilde{a}^{\rm in}, \quad (5a)$$

$$\dot{\tilde{b}} = -\frac{\gamma}{2}\tilde{b} + iG(\tilde{a}^\dagger e^{i(\omega_m+\Delta)t} + \tilde{a}e^{i(\omega_m-\Delta)t}) + \sqrt{\gamma}\tilde{b}^{\rm in}. \quad (5b)$$

Note that here we have used two newly defined noise operators $\tilde{a}^{\rm in} = a^{\rm in}e^{i\Delta t}$ and $\tilde{b}^{\rm in} = b^{\rm in}e^{i\omega_m t}$, possessing the same correlation functions.

We then proceed to discuss how to realize gain (or loss) in the mechanical resonator, in a pure quantum-mechanical way. To do so, we first assume that the cavity is resonant with the Stokes sideband of the driving laser, $\Delta = -\omega_m$, and invoke the rotating wave approximation (RWA) (which is justified in the limit of $\omega_m \gg \{G, \kappa, \gamma\}$) to obtain

$$\dot{\tilde{a}} = -\frac{\kappa}{2}\tilde{a} + iG\tilde{b}^\dagger + \sqrt{\kappa}\tilde{a}^{\rm in}, \quad (6a)$$

$$\dot{\tilde{b}} = -\frac{\gamma_m}{2}\tilde{b} + iG\tilde{a}^\dagger + \sqrt{\gamma}\tilde{b}^{\rm in}. \quad (6b)$$

Then under the condition that the cavity decay rate is much larger than the effective optomechanical coupling strength, i.e., $\kappa \gg \{G, \gamma_m\}$, one can further adiabatically eliminate the

cavity field to obtain

$$\tilde{a} = i\frac{2G}{\kappa}\tilde{b}^{\dagger} + \frac{2}{\sqrt{\kappa}}\tilde{a}^{\text{in}}. \tag{7}$$

Finally, following a substitution of Eq. (7) in Eq. (6b), we end up with the following equation which describes the effective dynamics of the mechanical resonator:

$$\dot{\tilde{b}} = \left(\frac{\Gamma}{2} - \frac{\gamma}{2}\right)\tilde{b} + i\sqrt{\Gamma}\tilde{a}^{\text{in}^{\dagger}} + \sqrt{\gamma}\tilde{b}^{\text{in}}. \tag{8}$$

Here, one should note the inclusion of the following two terms: first, $\Gamma = \frac{4G^2}{\kappa}$, which quantifies the amount of optomechanically induced gain in the mechanical resonator, and second, the cavity induced noise term $\sqrt{\Gamma}a^{\text{in}^{\dagger}}$, which helps to preserve the right commutation relation. On the other hand, when this cavity is resonant with the anti-Stokes sideband of the driving laser, i.e., $\Delta = \omega_m$, exercising a similar procedure, one obtains the following dynamical equation:

$$\dot{\tilde{b}} = -\left(\frac{\Gamma}{2} + \frac{\gamma}{2}\right)\tilde{b} + i\sqrt{\Gamma}\tilde{a}^{\text{in}} + \sqrt{\gamma}\tilde{b}^{\text{in}}, \tag{9}$$

where the same $\Gamma = \frac{4G^2}{\kappa}$ now corresponds to the optomechanically induced loss in the mechanical resonator, while the noise term denotes the same. Such derivation of optomechanically induced gain and loss can also be viewed in the following manner. Let us first say that the cavity is detuned to the Stokes sideband, i.e., $\Delta = -\omega_m$. Then, within the RWA, one obtains the interaction Hamiltonian of the form $H_I = -G(a^{\dagger}b^{\dagger} + ab)$ [see Eq. (6)]. Such a beam-splitter kind of interaction leads to a transition of any arbitrary state $|m, n\rangle$ (m and n being, respectively, the photon and phonon numbers of the cavity field and mechanical resonator) to $|m+1, n+1\rangle$. Further, subjected to a strong optical dissipation, this state $|m+1, n+1\rangle$ irreversibly loses a single photon and relaxes to $|m, n+1\rangle$. After eliminating the cavity field, this whole process becomes equivalent to a transition from $|n\rangle$ to $|n+1\rangle$, with an effective gain rate Γ. On the other hand, when the cavity is detuned to the anti-Stokes sideband, i.e., $\Delta = \omega_m$, one ends up with an interaction $H_I = -G(a^{\dagger}b + ab^{\dagger})$, that couples a state $|m, n\rangle$ to $|m+1, n-1\rangle$. Then, following an adiabatic elimination of the cavity field, one eventually gets a transition from $|n\rangle$ to $|n-1\rangle$, with a damping rate Γ.

III. ENTANGLEMENT IN $\mathcal{PT}$ SYMMETRIC BINARY SYSTEMS

We next couple two of these identical mechanical resonators, each characterized by a frequency (damping rate) ω_m (γ_m), via a mechanical coupling of strength J. Schematics of such a binary mechanical $\mathcal{PT}$ symmetric system and its optomechanical realization have been illustrated, respectively, in Figs. 1(a) and 1(b). Then, following the prescription as derived in Sec. II, we can write the effective dynamical equations as satisfied by each mechanical resonator, as follows:

$$\dot{b_1} = \left(\frac{\Gamma}{2} - \frac{\gamma}{2}\right)b_1 + iJb_2 + i\sqrt{\Gamma}a_1^{\text{in}^{\dagger}} + \sqrt{\gamma}b_1^{\text{in}}, \tag{10a}$$

$$\dot{b_2} = -\left(\frac{\Gamma}{2} + \frac{\gamma}{2}\right)b_2 + iJb_1 + i\sqrt{\Gamma}a_2^{\text{in}} + \sqrt{\gamma}b_2^{\text{in}}. \tag{10b}$$

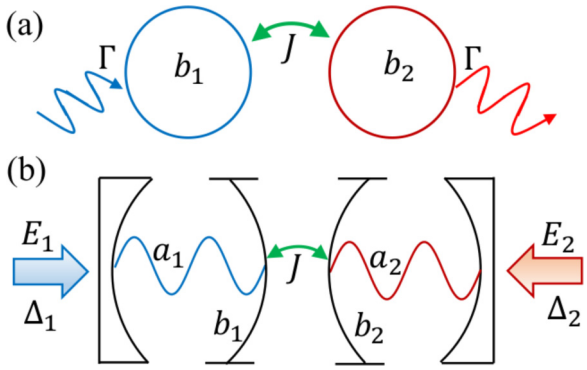

FIG. 1. (a) Schematic diagram of binary mechanical $\mathcal{PT}$ symmetric resonators, with optomechanically induced gain and loss. (b) Scheme for engineering mechanical gain and loss in an optomechanical platform. Here, two optomechanical cavities, respectively, driven at Stokes and anti-Stokes sidebands of the driving lasers, are coupled mutually via a mechanical interaction.

Here, b_1 and b_2 ($b_1^{\dagger}$ and $b_2^{\dagger}$) are the annihilation (creation) operators of the gain and lossy resonators, respectively, and Γ is the effective optomechanically induced gain or loss rate. Notably, here the interaction Hamiltonian between these two mechanical resonators is assumed to be of the form of $H_{\text{int}} = -J(b_1^{\dagger}b_2 + b_1b_2^{\dagger})$. Such an interaction could be generated from any common X-X type interaction as achieved in Refs. [65,66], under a RWA. The remaining parameters a_j^{in} and b_j^{in} ($j = 1, 2$), respectively, correspond to the vacuum input noises, acting on the cavity fields and the mechanical resonators. In the parameter regime, where the effective optomechanical coupling is strong enough, one can further discard the intrinsic mechanical damping as $\Gamma \gg \gamma$. However, to simulate the actual physical condition, we retain a finite damping $\gamma > 0$ throughout our calculations. It is also worthwhile to note that although we have assumed that the frequencies of both mechanical resonators, as well as their coupling rates to the cavity fields, are exactly the same, we find that slight deviations do not alter the overall conclusion of the obtained results. This makes our paper experimentally relevant.

By ignoring the quantum noises, we now recast Eq. (10) as $\dot{u}(t) = -iH_2u(t)$. Here, $u^T(t) = (q_1(t), p_1(t), q_2(t), p_2(t))$ is the state vector, written in terms of the dimensionless CV quadrature operators $q_j \equiv (b_j + b_j^{\dagger})/\sqrt{2}$ and $p_j \equiv (b_j - b_j^{\dagger})/i\sqrt{2}$ (with $j = 1, 2$), where H_2 is the non-Hermitian Hamiltonian, given by

$$H_2 = i\begin{pmatrix} \frac{\Gamma}{2} & 0 & 0 & -J \\ 0 & \frac{\Gamma}{2} & J & 0 \\ 0 & -J & -\frac{\Gamma}{2} & 0 \\ J & 0 & 0 & -\frac{\Gamma}{2} \end{pmatrix}. \tag{11}$$

It is then easy to verify that under the simultaneous $\mathcal{PT}$ operation the Hamiltonian H_2 remains invariant, i.e., $[\mathcal{PT}, H_2] = 0$. Now, in order to study the $\mathcal{PT}$ phase transition, we first diagonalize the Hamiltonian and find the eigenfrequencies:

$$\omega_{\pm} = \pm\sqrt{J^2 - \left(\frac{\Gamma}{2}\right)^2}, \tag{12}$$

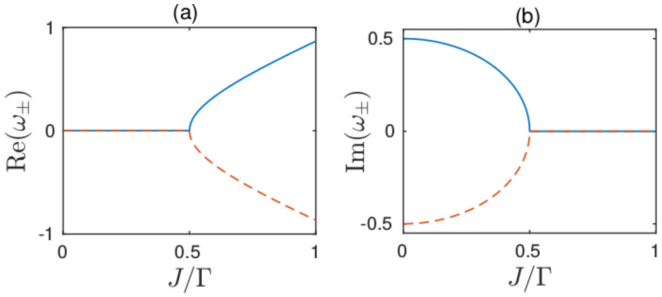

FIG. 2. (a) The real and (b) the imaginary parts of $\omega_\pm$ vs the normalized coupling coefficient J/Γ. The system exhibits an exceptional point (of order 2) at $J = \frac{\Gamma}{2}$.

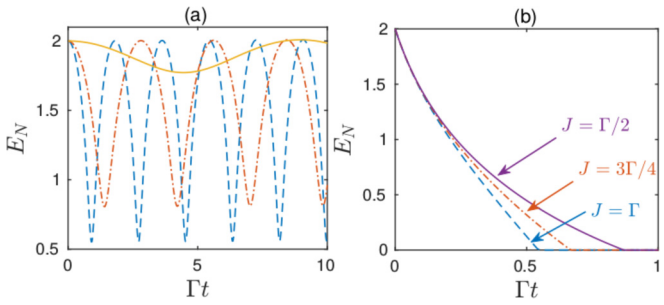

FIG. 3. Entanglement evolution between the gain and loss resonators (a) in the absence and (b) in the presence of noises. The parameters used are $\Gamma = 1$ and $\gamma = 10^{-3}$. In panel (a) the blue (dashed), red (dash-dotted), and yellow (solid) lines, respectively, correspond to $J = \Gamma$, 0.75Γ, and 0.53Γ.

where the real and imaginary parts, respectively, correspond to the effective frequency and dissipation of the mechanical resonator. Then, as can be seen from Eq. (12), respectively, for $J > \Gamma/2$ and $J < \Gamma/2$ there exist two distinct phases: one that includes all the real eigenvalues, namely, a $\mathcal{PT}$ symmetric phase, and the other, which possesses purely imaginary eigenvalues, namely, a broken $\mathcal{PT}$ symmetric phase. The critical coupling strength which separates these two phases is marked by $J_{c_2} = \Gamma/2$. An exact situation can be found in Fig. 2, where we depict the eigenfrequencies as a function of the normalized coupling strength J/Γ. Also, we observe that this same J_{c_2} marks the exceptional point (of order 2) of this system where the two eigenvalues coalesce. It should be noted that in order to obtain a closed expression for the $\mathcal{PT}$ symmetric condition we have not included the mechanical damping γ as justified by the fact that $\Gamma \gg \gamma$. However, in all our numerical calculations, we do consider a finite degree of mechanical damping γ.

Physically, the emergence of such an EP refers to the situation where the mechanical coupling rate J gets exactly balanced with the respective mechanical heating and cooling rates Γ. Then, for all $J > \frac{\Gamma}{2}$ there is a coherent exchange of energy between these two resonators which corresponds to the $\mathcal{PT}$ symmetric phase. However, as soon as the coupling becomes weak enough to support the energy exchange, i.e., for any $J < \frac{\Gamma}{2}$, there is a localization of energy in the the passive resonator which in turn leads to the breaking of $\mathcal{PT}$ symmetry.

Next, we take the full quantum noises into account and rewrite Eq. (10) in a more compact form: $\dot{u}(t) = Au(t) + n(t)$. Here, $u(t)$ is the same CV state vector, $A = -iH_2$ is the drift matrix, and $n^T(t) = (\sqrt{\Gamma}Y_1^{\rm in} + \sqrt{\gamma}Q_1^{\rm in}, \sqrt{\Gamma}X_1^{\rm in} + \sqrt{\gamma}P_1^{\rm in}, -\sqrt{\Gamma}Y_2^{\rm in} + \sqrt{\gamma}Q_2^{\rm in}, \sqrt{\Gamma}X_2^{\rm in} + \sqrt{\gamma}P_2^{\rm in})$ is the matrix of corresponding noises. The input noise quadratures, as used in $n^T(t)$, are, respectively, defined as follows: $X_c^{\rm in} \equiv (a_c^{\rm in} + a_c^{\rm in^\dagger})/\sqrt{2}$, $Y_c^{\rm in} \equiv (a_c^{\rm in} - a_c^{\rm in^\dagger})/i\sqrt{2}$, and $Q_c^{\rm in} \equiv (b_c^{\rm in} + b_c^{\rm in^\dagger})/\sqrt{2}$, $P_c^{\rm in} \equiv (b_c^{\rm in} - b_c^{\rm in^\dagger})/i\sqrt{2}$ where $c = 1, 2$. A formal solution of this Langevin equation reads as $u(t) = e^{At}u(0) + \int_0^t ds e^{A(t-s)}n(s)$. Then, for a stable solution one requires all the eigenvalues of A with negative real parts. In what follows, we find that one can have such solutions only when the system remains in the $\mathcal{PT}$ symmetric phase.

We further note that owing to the above linearized dynamics and zero-mean Gaussian nature of the quantum noises the system retains its Gaussian characteristics. In turn, one can adopt the standard covariance matrix (CM) formalism to fully describe the system [67]. Let $V(t)$ be the CM with each element defined as $V_{ij}(t) = \langle u_i(t)u_j(t) + u_j(t)u_i(t)\rangle/2$. Then, one has the following equation of motion as satisfied by the CM:

$$\dot{V}(t) = AV(t) + V(t)A^T + D. \tag{13}$$

Here, $D = [\frac{\Gamma}{2} + \gamma(n_{\rm th} + \frac{1}{2})]{\rm diag}(1, 1, 1, 1)$ is the matrix of the noise correlations, obtained under the Markovian assumption, and $\langle n_i(t)n_j(t') + n_j(t')n_i(t)\rangle/2 = \delta(t - t')D_{ij}$.

Equation (13) is an inhomogeneous first-order differential equation which can be solved numerically with a proper initial condition (please see the Appendix for an analytical solution). As studying the quantum correlation is our primary concern, here, we consider this input state to be a generic CV entangled state, i.e., a two-mode squeezed state $|z\rangle = e^{r(b_1^\dagger b_2^\dagger - b_1 b_2)}|0, 0\rangle$ with r being the squeezing parameter. In order to realize such states in optomechanical oscillators, one may look into various striking proposals in Refs. [68–71]. The formal solution of Eq. (13) takes the following form of $V(.)$:

$$V \equiv \begin{pmatrix} V_G & V_{GL} \\ V_{GL}^T & V_L \end{pmatrix}, \tag{14}$$

where V_G, V_L, and V_{GL} are 2×2 block matrices, respectively, corresponding to the local covariance matrices of resonators 1 and 2, and the nonlocal correlation between them. One can, then, gauge the degree of quantum entanglement by calculating the so-called logarithmic negativity E_N, defined as $E_N = \max[0, -\ln 2\nu^-]$ [72,73]. Here $\nu^- \equiv 2^{-1/2}[\Sigma(V) - \sqrt{\Sigma(V)^2 - 4{\rm det}V}]^{1/2}$ is the smallest symplectic eigenvalue of the partial transpose of V with $\Sigma(V) \equiv {\rm det}(V_G) + {\rm det}(V_L) - 2{\rm det}(V_{GL})$.

In Fig. 3(a) we first show the time evolution of the quantum entanglement in the absence of any noises. One can see that when the system is in the $\mathcal{PT}$ symmetric phase the entanglement oscillates periodically. This oscillation could be attributed to the nature of the eigenvalues $\pm i\sqrt{J^2 - J_{c_2}^2}$ of A, as obtained for $J > J_{c_2}$ (see the Appendix for further discussion). However, as we approach the EP, we notice a

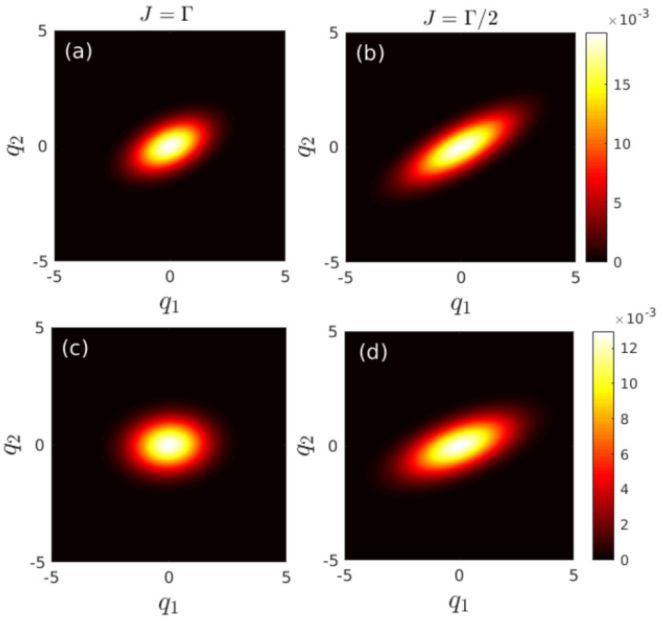

FIG. 4. Time evolution of Wigner functions $W(q_1, q_2)^{p_1=0}_{p_2=0}$, respectively, at $\Gamma t = 0.5$ (upper two panels) and 0.75 (bottom two panels).

lesser oscillation with a longer time period. Finally, in the close vicinity of the EP ($J \to J_{c_2}$), the entanglement dynamics almost "freezes out," i.e., it takes a longer period to complete one such oscillation. In Fig. 3(b), we show the same entanglement evolution, but now taking the quantum noises into account. One can see that as soon as noise is introduced into the system the entanglement quickly decays to zero, a typical ESD-like behavior. However, a more notable feature is the delayed death of entanglement, as achieved via pushing the system towards the EP.

To further support this conclusion, in Fig. 4 we compare the two-mode Wigner functions for two different coupling strengths, at two different times. One can see that at $\Gamma t = 0.5$ both these $W(q_1, q_2)^{p_1=0}_{p_2=0}$ exhibit a squeezinglike behavior which is sufficient to ensure the onset of entanglement between these two mechanical oscillators. However, at a subsequent time $\Gamma t = 0.75$, one finds that the $W(q_1, q_2)^{p_1=0}_{p_2=0}$ corresponding to $J = \Gamma$ almost loses its squeezing characteristic, while the other still retains it with a finite degree. Moreover, it is also important to note that for both these coupling strengths the Wigner functions remain localized in the phase space, i.e., there is no abrupt stretching associated with $W(q_1, q_2)^{p_1=0}_{p_2=0}$ that could push the system towards instability.

IV. ENTANGLEMENT IN $\mathcal{PT}$ SYMMETRIC TERNARY SYSTEMS

Motivated by these results, we now extend this same strategy to the higher-order exceptional points. A possible realization that supports an exceptional point of order 3 (EP3) would be a ternary mechanical system where the gain and lossy resonators are being separated by a neutral one (see Fig. 5). Then, proceeding in a similar manner, one can write

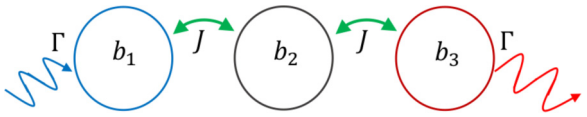

FIG. 5. Schematic illustration of the $\mathcal{PT}$ symmetric ternary mechanical setup. Here, the side resonators are subjected to equivalent gain and loss, while the middle one is neutral.

the following equation of motion, as satisfied by each mechanical resonator:

$$\dot{b_1} = \left(\frac{\Gamma}{2} - \frac{\gamma}{2}\right) b_1 + iJb_2 + i\sqrt{\Gamma} a_1^{\text{in}^\dagger} + \sqrt{\gamma} b_1^{\text{in}}, \tag{15a}$$

$$\dot{b_2} = -\frac{\gamma}{2} b_2 + iJb_1 + iJb_3 + \sqrt{\gamma} b_2^{\text{in}}, \tag{15b}$$

$$\dot{b_3} = -\left(\frac{\Gamma}{2} + \frac{\gamma}{2}\right) b_3 + iJb_2 + i\sqrt{\Gamma} a_2^{\text{in}} + \sqrt{\gamma} b_3^{\text{in}}. \tag{15c}$$

Here, b_1, b_2, and b_3 ($b_1^\dagger$, $b_2^\dagger$, and $b_3^\dagger$) refer to the annihilation (creation) operators of the gain, neutral, and lossy resonators, respectively, while the other parameters remain unaltered with their previous descriptions. Then, in the absence of any noises, one can have the following cubic algebraic equation as obeyed by each of these eigenfrequencies ω_n ($n \in \{-1, 0, 1\}$):

$$\omega_n \left(\omega_n^2 + \frac{\Gamma^2}{4} - 2J^2\right) = 0. \tag{16}$$

It is evident that for a critical coupling strength $J_{c_3} = \frac{\Gamma}{2\sqrt{2}}$ all three eigenfrequencies merge at $\omega_n = 0$. This characteristic feature of the EP3 has been pictorially demonstrated in Fig. 6, where we show the dependence of the eigenfrequencies on the normalized coupling strength J/Γ.

Now, to take this discussion further, we consider the case of tripartite entanglement between these three mechanical resonators, under the $\mathcal{PT}$ symmetric scenario. The measurement of such complicated multipartite entanglement goes as follows. Let us first define the following linear combinations of the quadrature variances:

$$x \equiv h_1 q_1 + h_2 q_2 + h_3 q_3, \tag{17a}$$

$$y \equiv g_1 p_1 + g_2 p_2 + g_3 p_3, \tag{17b}$$

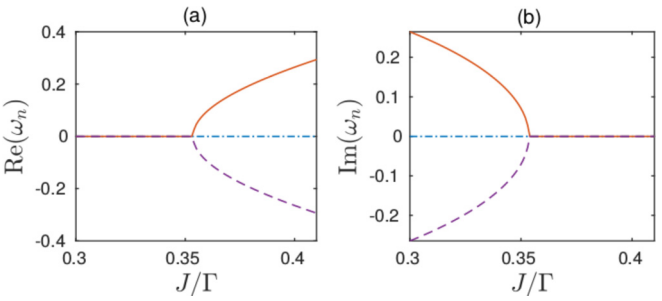

FIG. 6. (a) The real and (b) the imaginary parts of ω_n as a function of the normalized coupling coefficient J/Γ. The three eigenfrequencies merge at $J = \frac{\Gamma}{2\sqrt{2}}$, exhibiting a third-order exceptional point.

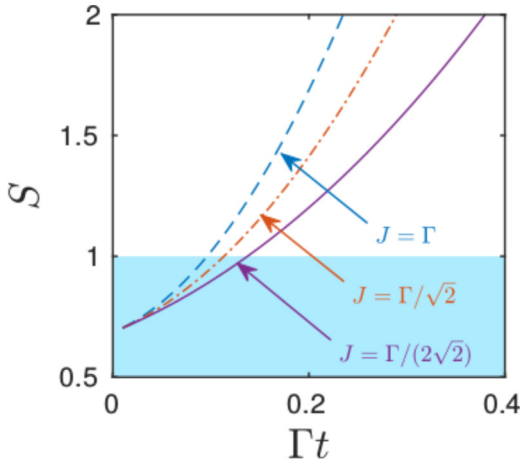

FIG. 7. Time evolution of the nonseparability criteria S, for three different coupling strengths. The shaded area guarantees the presence of genuine tripartite entanglement. The parameters used are the same as those in Fig. 3.

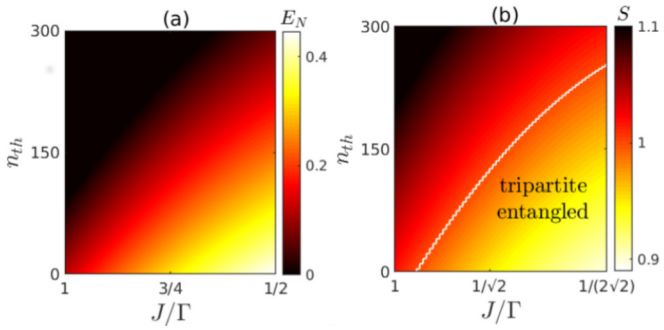

FIG. 8. (a) Bipartite and (b) tripartite entanglement measures, as a function of the normalized coupling J/Γ and the number of thermal phonons $n_{\rm th}$. The times corresponding to each snapshot are, respectively, (a) $\Gamma t = 0.5$ and (b) 0.1. In Fig. 8(b), the white line separates between two distinct regimes of genuine tripartite entanglement and full tripartite inseparability.

where q_1, q_2, and q_3 (p_1, p_2, and p_3) are the position (momentum) operators of the gain, neutral, and lossy resonators, respectively, while h_k and g_k are any arbitrary real parameters. Then, following the prescription as proposed in Refs. [74–76], we employ the nonseparability measurement

$$S = \langle(\Delta x)^2\rangle + \langle(\Delta y)^2\rangle. \tag{18}$$

The three-party state is then said to be *genuinely tripartite entangled* if and only if it negates the following single inequality:

$$S \geqslant \min\{|h_3 g_3| + |h_1 g_1 + h_2 g_2|, \\ |h_2 g_2| + |h_1 g_1 + h_3 g_3|, |h_1 g_1| + |h_2 g_2 + h_3 g_3|\}, \tag{19}$$

whereas only the violation of any of these inequalities

$$S \geqslant (|h_k g_k| + |h_l g_l + h_m g_m|), \tag{20}$$

for a given permutation of $\{k, l, m\}$ of $\{1, 2, 3\}$, guarantees a *full tripartite inseparability*. These classes of nonseparabilities may sound equivalent, but as pointed out by Teh and Reid [75] they remain indistinguishable only for pure quantum states, while for mixed states meeting the full inseparability criteria does not suffice to claim multipartite entanglement. In order to numerically evaluate the bounds of Eqs. (19) and (20), we now consider the set of parameters $h_1 = g_1 = 1$ and $g_2 = g_3 = -h_2 = -h_3 = 1/\sqrt{2}$. The reason behind such a particular combination is $[q_1 - (q_2 + q_3)/\sqrt{2}, p_1 + (p_2 + p_3)/\sqrt{2}] = 0$, which allows us to have an arbitrary good degree of violation of (19). Then, one has to fulfill $S < 1$ to ensure the emergence of genuine tripartite entanglement, while $S < 2$ will suffice to confirm at least full tripartite inseparability.

Figure 7 depicts the time evolution of S, starting from a CV Greenberger-Horne-Zeilinger state with the squeezing parameters r_1 and r_2 being equal to 1 [74]. It is observed that, with the inclusion of quantum noise, the tripartite state quickly suffers a sudden death of (genuine tripartite) entanglement, followed by a fully tripartite inseparable state. However, it is remarkable to note that at the EP3 such a three-party state loses entanglement more slowly as compared to any other points in the unbroken $\mathcal{PT}$ symmetric phase. One may also notice that by operating near the EP3 it is possible to prolong the time pertaining to a full tripartite inseparable state.

Finally, in Fig. 8 we examine the effect of thermal noise on the bipartite [Fig. 8(a)] and tripartite entanglement [Fig. 8(b)] evolution. As expected, the degradation of quantum entanglement with an increasing thermal phonon is observed. However, it is worthwhile to note that the available bipartite (tripartite) entanglement achieved in the close vicinity of the EPs (EP3) is fairly robust. To experimentally assess these entanglements, one needs to measure all ten independent entries of the correlation matrix. A feasible way to do this is to couple each mechanical resonator to an ancilla cavity via an optomechanical interaction. Then, if one sets the input cavity detuning to the red sideband of the driving laser, one can enhance the so-called beam-splitter or state transfer type of interaction, where the mechanical field can be exactly mapped to an optical field. This enables us to measure all the required second moments in the correlation matrix by homodyning the output cavity fields. Also, one can exercise a similar homodyne detection technique to measure the tripartite nonseparability criteria.

V. CONCLUSION

In conclusion, we have performed a systematic study to unravel the relation between death of entanglement and the phenomenon of exceptional points. The architectures that we have specifically focused on are, essentially, binary and ternary mechanical $\mathcal{PT}$ symmetric systems with optomechanically induced gain and loss. Our paper shows that a substantial delay in sudden death of entanglement is possible at exceptional points, respectively, of orders 2 and 3. It is also shown that near the EPs the available entanglement survives to a much higher degree of thermal phonons. These findings may pave the ways for exploiting $\mathcal{PT}$ symmetric devices as novel means to control the entanglement dynamics in different QIP protocols. It is also worthwhile to note that our approach could, in principle, be applied in various photonic and phononic $\mathcal{PT}$ symmetric systems, with engineered gain and loss mechanisms. Further efforts along this direction include

the investigation of quantum entanglement in the broken $\mathcal{PT}$ symmetric regime, where the effect of gain saturation must be treated with care.

ACKNOWLEDGMENT

S.C. would like to acknowledge Ministry of Human Resource Development, Government of India for providing financial support for his research.

APPENDIX

Here, we aim to find an explicit analytical solution pertaining to each of the variances in the correlation matrix $V(t)$. We first consider that there are no quantum noises acting on the system. Then, under the $\mathcal{PT}$ symmetric condition, the solutions can be written (neglecting the mechanical damping γ) as follows:

$$\langle q_1^2\rangle = \frac{\cosh(2r)}{2}\left[\frac{\Gamma}{2\omega_+}\sin(2\omega_+ t) - \frac{\Gamma^2}{4\omega_+^2}\cos(2\omega_+ t) + \frac{J^2}{\omega_+^2}\right], \tag{A1a}$$

$$\frac{\langle q_1 p_1 + p_1 q_1\rangle}{2} = \frac{\sinh(2r)}{2}\left\{-\frac{J}{2\omega_+}\sin(2\omega_+ t) - \frac{\Gamma J}{2\omega_+^2}\left[\cos(2\omega_+ t) - 1\right]\right\}, \tag{A1b}$$

$$\langle p_1^2\rangle = \frac{\cosh(2r)}{2}\left[\frac{\Gamma}{2\omega_+}\sin(2\omega_+ t) - \frac{\Gamma^2}{4\omega_+^2}\cos(2\omega_+ t) + \frac{J^2}{\omega_+^2}\right], \tag{A1c}$$

$$\langle q_2^2\rangle = \frac{\cosh(2r)}{2}\left[-\frac{\Gamma}{2\omega_+}\sin(2\omega_+ t) - \frac{\Gamma^2}{4\omega_+^2}\cos(2\omega t) + \frac{J^2}{\omega_+^2}\right], \tag{A1d}$$

$$\frac{\langle q_2 p_2 + p_2 q_2\rangle}{2} = \frac{\sinh(2r)}{2}\left\{\frac{J}{2\omega_+}\sin(2\omega_+ t) + \frac{\Gamma J}{2\omega_+^2}\left[1 - \cos(2\omega_+ t)\right]\right\}, \tag{A1e}$$

$$\langle p_2^2\rangle = \frac{\cosh(2r)}{2}\left[-\frac{\Gamma}{2\omega_+}\sin(2\omega_+ t) - \frac{\Gamma^2}{2\omega_+^2}\cos(2\omega_+ t) + \frac{J^2}{\omega_+^2}\right], \tag{A1f}$$

$$\frac{\langle q_1 q_2 + q_2 q_1\rangle}{2} = \frac{\sinh(2r)}{2\omega_+^2}\left[J^2\cos(2\omega_+ t) - \frac{\Gamma^2}{4}\right], \tag{A1g}$$

$$\frac{\langle q_1 p_2 + p_2 q_1\rangle}{2} = \frac{\Gamma J\cosh(2r)}{4\omega_+^2}\left[\cos(2\omega_+ t) - 1\right], \tag{A1h}$$

$$\frac{\langle p_1 q_1 + q_1 p_1\rangle}{2} = \frac{\Gamma J\cosh(2r)}{4\omega_+^2}\left[1 - \cos(2\omega_+ t)\right], \tag{A1i}$$

$$\frac{\langle p_1 p_2 + p_2 p_1\rangle}{2} = -\frac{\sinh(2r)}{2} - \frac{J^2\sinh(2r)}{2\omega_+^2}\left[\cos(2\omega_+ t) - 1\right]. \tag{A1j}$$

It can be seen that all these variances undergo a periodic oscillation with a time period $T = \pi/\sqrt{J^2 - \Gamma^2/4}$ (similar to Ref. [35]) and at the EP they all return to their initial states. Such characteristic features of the $\mathcal{PT}$ symmetric phase have also been mapped on the entanglement evolution. It is found that as the EP is approached the oscillations become less, and the tendency to retain the initial entanglement becomes high. To get further insight into this CV entanglement, we now evaluate the collective variances of the mechanical quadratures, as given below:

$$\mathrm{Var}(q_1 - q_2) = \frac{\cosh(2r)}{\omega_+^2}\left[J^2 - \frac{\Gamma^2}{4}\cos(2\omega_+ t)\right] - \frac{\sinh(2r)}{\omega_+^2}\left[J^2\cos(2\omega_+ t) - \frac{\Gamma^2}{4}\right]. \tag{A2}$$

It can be found that for an EPR-type correlation [$\mathrm{Var}(q_1 - q_2) = e^{-2r}$] one must have $\cos(2\omega_+ t) = 0$, i.e., $J = \Gamma/2$. This clearly signifies the presence of the two-mode squeezed state and thereby a $2r$ degree of entanglement at the EP [see Fig. 3(a)].

We next take the quantum noises into account. Here, these equations become so complicated that it is extremely difficult to present the variances in simple forms. However, evaluating explicitly at the EP gives us the following form of the collective variance:

$$\mathrm{Var}(q_1 - q_2)\Big|_{J=\frac{\Gamma}{2}} = e^{-2r} + \Gamma t + \frac{\Gamma^2 t^2}{2}e^{2r} + \frac{\Gamma^3 t^3}{6}. \tag{A3}$$

Equation (A3) clearly discriminates the unitary time evolution of the variances and the diffusion induced by the quantum noise. Hence, we observe a quick decay of entanglement [Fig. 3(b)] when exposed to the quantum noises.

[1] C. M. Bender and S. Boettcher, Phys. Rev. Lett. **80**, 5243 (1998).

[2] C. M. Bender, D. C. Brody, and H. F. Jones, Phys. Rev. Lett. **89**, 270401 (2002).

[3] R. El-Ganainy, K. G. Makris, M. Khajavikhan, Z. H. Musslimani, S. Rotter, and D. N. Christodoulides, Nat. Phys. **14**, 11 (2018).

[4] W. D. Heiss, J. Phys. A **45**, 444016 (2012).

[5] K. G. Makris, R. El-Ganainy, D. N. Christodoulides, and Z. H. Musslimani, Phys. Rev. Lett. **100**, 103904 (2008).

[6] Z. H. Musslimani, K. G. Makris, R. El-Ganainy, and D. N. Christodoulides, Phys. Rev. Lett. **100**, 030402 (2008).

[7] A. Guo, G. J. Salamo, D. Duchesne, R. Morandotti, M. Volatier-Ravat, V. Aimez, G. A. Siviloglou, and D. N. Christodoulides, Phys. Rev. Lett. **103**, 093902 (2009).

[8] C. E. Rüter, K. G. Markis, R. El.-Ganainy, D. N. Christodoulides, M. Segev, and D. Kip, Nat. Phys. **6**, 192 (2010).

[9] A. Regensburger, C. Bersch, M.-A. Miri, G. Onishchukov, D. N. Christodoulides, and U. Peschel, Nature (London) **488**, 167 (2012).

[10] B. Peng, S. K. Özdemir, F. Lei, F. Monifi, M. Gianfreda, G. L. Long, S. Fan, F. Nori, C. M. Bender, and L. Yang, Nat. Phys. **10**, 394 (2014).

[11] L. Feng, Z. J. Wong, R.-M. Ma, Y. Wang, and X. Zhang, Science **346**, 972 (2014).

[12] H. Hodaei, M.-A. Miri, M. Heinrich, D. N. Christodoulides, and M. Khajavikhan, Science **346**, 975 (2014).

[13] H. Hodaei, A. U. Hassan, W. E. Hayenga, M. A. Miri, D. N. Christodoulides, and M. Khajavikhan, Opt. Lett. **41**, 3049 (2016).

[14] B. Peng, S. K. Özdemir, M. Liertzer, W. Chen, J. Kramer, H. Yilmaz, J. Wiersig, S. Rotter, and L. Yang, Proc. Natl. Acad. Sci. USA **113**, 6845 (2016).

[15] Z. Lin, H. Ramezani, T. Eichelkraut, T. Kottos, H. Cao, and D. N. Christodoulides, Phys. Rev. Lett. **106**, 213901 (2011).

[16] S. Longhi, J. Phys. A **44**, 485302 (2011).

[17] L. Feng, Y.-L. Xu, W. S. Fegadolli, M.-H. Lu, J. E. B. Oliveira, V. R. Almeida, Y.-F. Chen, and A. Scherer, Nat. Mater. **12**, 108 (2013).

[18] J. Wiersig, Phys. Rev. Lett. **112**, 203901 (2014)

[19] H. Hodaei, A. U. Hassan, S. Wittek, H. Garcia-Gracia, R. El-Ganainy, D. N. Christodoulides, and M. Khajavikhan, Nature (London) **548**, 187 (2017).

[20] W. Chen, Ş. K. Özdemir, G. Zhao, J. Wiersig, and L. Yang, Nature (London) **548**, 192 (2017).

[21] T. Goldzak, A. A. Mailybaev, and N. Moiseyev, Phys. Rev. Lett. **120**, 013901 (2018).

[22] P. Miao, Z. Zhang, J. Sun, W. Walasik, S. Longhi, N. M. Litchinitser, and L. Feng, Science **353**, 464 (2016).

[23] C. Hang, G. Huang, and V. V. Konotop, Phys. Rev. Lett. **110**, 083604 (2013).

[24] D. Haag, D. Dast, A. Löhle, H. Cartarius, J. Main, and G. Wunner, Phys. Rev. A **89**, 023601 (2014).

[25] H. Cartarius and G. Wunner, Phys. Rev. A **86**, 013612 (2012).

[26] H. Jing, S. K. Özdemir, X.-Y. Lü, J. Zhang, L. Yang, and F. Nori, Phys. Rev. Lett. **113**, 053604 (2014).

[27] X.-W. Xu, Y.-X. Liu, C.-P. Sun, and Y. Li, Phys. Rev. A **92**, 013852 (2015).

[28] X.-Y. Lü, H. Jing, J.-Y. Ma, and Y. Wu, Phys. Rev. Lett. **114**, 253601 (2015).

[29] F. Quijandría, U. Naether, S. K. Özdemir, F. Nori, and D. Zueco, Phys. Rev. A **97**, 053846 (2018).

[30] Y. Ashida, S. Furukawa, and M. Ueda, Nat. Commun. **8**, 15791 (2017).

[31] S.-L. Chen, G.-Y. Chen, and Y.-N. Chen, Phys. Rev. A **90**, 054301 (2014).

[32] H. Xu, D. Mason, L. Jiang, and J. G. E. Harris, Nature (London) **537**, 80 (2016).

[33] J. Doppler, A. A. Mailybaev, J. Böhm, U. Kuhl, A. Girschik, F. Libisch, T. J. Milburn, P. Rabl, N. Moiseyev, and S. Rotter, Nature (London) **537**, 76 (2016).

[34] B. Gardas, S. Deffner, and A. Saxena, Phys. Rev. A **94**, 040101(R) (2016).

[35] K. Kawabata, Y. Ashida, and M. Ueda, Phys. Rev. Lett. **119**, 190401 (2017).

[36] G. S. Agarwal and K. Qu, Phys. Rev. A **85**, 031802(R) (2012).

[37] K. V. Kepesdis, T. J. Milburn, J. Huber, K. G. Makris, S. Rotter, and P. Rabl, New J. Phys. **18**, 095003 (2016).

[38] H.-K. Lau and A. A. Clerk, Nat. Commun. **9**, 4320 (2018).

[39] M. Zhang, W. Sweeney, C. W. Hsu, L. Yang, A. D. Stone, and L. Jiang, Phys. Rev. Lett. **123**, 180501 (2019).

[40] S. Vashahri-Ghamsari, B. He, and M. Xiao, Phys. Rev. A **96**, 033806 (2017).

[41] S. Vashahri-Ghamsari, B. He, and M. Xiao, Phys. Rev. A **99**, 023819 (2019).

[42] R. Horodecki, P. Horodecki, M. Horodecki, and K. Horodecki, Rev. Mod. Phys. **81**, 865 (2009).

[43] T. Yu and J. H. Eberly, Science **323**, 598 (2009).

[44] J. Laurat, K. S. Choi, H. Deng, C. W. Chou, and H. J. Kimble, Phys. Rev. Lett. **99**, 180504 (2007).

[45] M. P. Almeida, F. de Melo, M. Hor-Meyll, A. Salles, S. P. Walborn, P. H. Souto Ribeiro, and L. Davidovich, Science **316**, 579 (2007).

[46] C. Cormick and J. P. Paz, Phys. Rev. A **78**, 012357 (2008).

[47] J. P. Paz and A. J. Roncaglia, Phys. Rev. Lett. **100**, 220401 (2008).

[48] A. S. Coelho, F. A. S. Barbosa1, K. N. Cassemiro, A. S. Villar, M. Martinelli, and P. Nussenzveig, Science **326**, 823 (2009).

[49] J. Preskill, Proc. R. Soc. A **454**, 385 (1998).

[50] P. W. Shor, Phys. Rev. A **52**, R2493(R) (1995).

[51] A. R. P. Rau, M. Ali, and G. Alber, Europhys. Lett. **82**, 40002 (2008).

[52] A. Sing, S. Pradyumna, A. R. P. Rau, and U. Sinha, J. Opt. Soc. Am. B **34**, 681 (2017).

[53] L. Viola, E. Knill, and S. Lloyd, Phys. Rev. Lett. **82**, 2417 (1999).

[54] M. J. Biercuk, H. Uys, A. P. VanDevender, N. Shiga, W. M. Itano, and J. J. Bollinger, Nature (London) **458**, 996 (2009).

[55] D. A. Lidar, I. L. Chuang, and K. B. Whaley, Phys. Rev. Lett. **81**, 2594 (1998).

[56] P. G. Kwiat, A. J. Berglund, J. B. Altepeter, and A. G. White, Science **290**, 498 (2000).

[57] P. Facchi, D. A. Lidar, and S. Pascazio, Phys. Rev. A **69**, 032314 (2004).

[58] S. Maniscalco, F. Francica, R. L. Zaffino, N. Lo Gullo, and F. Plastina, Phys. Rev. Lett. **100**, 090503 (2008).

[59] J.-C. Lee, H.-T. Lim, K.-H. Hong, Y.-C. Jeong, M. S. Kim, and Y.-H. Kim, Nat. Commun. **5**, 4522 (2014).

[60] Y. S. Kim, Y. W. Cho, Y.-S. Ra, and Y.-H. Kim, Opt. Express **17**, 11978 (2009).

[61] J. C. Lee, Y. C. Jeong, Y. S. Kim, and Y. H. Kim, Opt. Express **19**, 16309 (2011).

[62] Q. Sun, M. Al-Amri, L. Davidovich, and M. S. Zubairy, Phys. Rev. A **82**, 052323 (2010).

[63] W. Li, C. Li, and H. Song, Phys. Rev. A **95**, 023827 (2017).

[64] M. Aspelmeyer, T. J. Kippenberg, and F. Marquardt, Rev. Mod. Phys. **86**, 1391 (2014).

[65] M. Spletzer, A. Raman, A. Q. Wu, X. F. Xu, and R. Reifenberger, Appl. Phys. Lett. **88**, 254102 (2006).

[66] E. Gil-Santos, D. Ramos, V. Pini, M. Calleja, and J. Tamayo, Appl. Phys. Lett. **98**, 123108 (2011).

[67] S. L. Braunstein and P. van Loock, Rev. Mod. Phys. **77**, 513 (2005).
[68] R. Riedinger, A. Wallucks, I. Marinković, C. Löschnauer, M. Aspelmeyer, S. Hong, and S. Gröblacher, Nature (London) **556**, 473 (2018).
[69] C. F. Ockeloen-Korppi, E. Damaskägg, J.-M. Pirkkalainen, A. A. Clerk, F. Massel, M. J. Woolley, and M. A. Sillanpää, Nature (London) **556**, 478 (2018).
[70] I. Marinković, A. Wallucks, R. Riedinger, S. Hong, M. Aspelmeyer, and S. Gröblacher, Phys. Rev. Lett. **121**, 220404 (2018).
[71] K. Børkje, A. Nunnenkamp, and S. M. Girvin, Phys. Rev. Lett. **107**, 123601 (2011).
[72] G. Vidal and R. F. Werner, Phys. Rev. A **65**, 032314 (2002).
[73] G. Adesso, A. Serafini, and F. Illuminati, Phys. Rev. A **70**, 022318 (2004).
[74] P. van Loock and A. Furusawa, Phys. Rev. A **67**, 052315 (2003).
[75] R. Y. Teh and M. D. Reid, Phys. Rev. A **90**, 062337 (2014).
[76] E. A. R. Gonzalez, A. Borne, B. Boulanger, J. A. Levenson, and K. Bencheikh, Phys. Rev. Lett. **120**, 043601 (2018).